HHS Public Access

Author manuscript

Spine J. Author manuscript; available in PMC 2017 November 01.

Published in final edited form as:

Spine J. 2016 March ; 16(3): 291–298. doi:10.1016/j.spinee.2015.08.041.

Early Magnetic Resonance Imaging Biomarkers to Predict Local Control after High Dose Stereotactic Body Radiotherapy for Patients with Sarcoma Spine Metastases

Daniel E. Spratt, MD[*,#], **Julio A. Perez, MD**[†], **Jonathan E. Leeman, MD**[*], **Naamit K. Gerber, MD**[*], **Michael Folkert, MD/PhD**[*,Ψ], **Neil K. Taunk, MD**[*], **Kaled M. Alektiar, MD**[*], **Sasan Karimi, MD**[†], **John K. Lyo, MD**[†], **William D. Tap, MD**[§], **Mark H. Bilsky, MD**[‡], **Ilya Laufer, MD**[‡], **Yoshiya Yamada, MD**[*], and **Joseph R. Osborne, MD/PhD**[†]

[†]Department of Radiology, Memorial Sloan Kettering Cancer Center, New York, New York

[Ψ]Department of Radiation Oncology, UT Southwestern, Dallas, Texas

[*]Department of Radiation Oncology, Memorial Sloan Kettering Cancer Center, New York, New York

[‡]Department of Neurosurgery, Memorial Sloan Kettering Cancer Center, New York, New York

[§]Department of Medical Oncology, Memorial Sloan Kettering Cancer Center, New York, New York

Abstract

Background Context—Recent advances in image guidance and stereotactic body radiotherapy (SBRT) have resulted in unprecedented local control for spinal metastases of all histologies. However, little is known about early imaging biomarkers of local control.

Purpose—To identify early MRI biomarkers to predict local control after SBRT for patients with sarcoma spine metastases.

Study Design/Setting—Retrospective case series at a large tertiary cancer center.

Patient Sample—From 2011 to 2014, nine consecutive patients with 12 metastatic sarcoma lesions to the spine were treated with SBRT and underwent evaluation with DCE-MRI both pre- and post-SBRT.

Outcome Measure—Changes in perfusion metrics, including the wash-in rate constant (Ktrans), plasma volume (Vp), composite multi-parametric MRI (mpMRI) score, bi-dimensional tumor size, and a graded response assessment were performed and correlated to local control.

[#]**Corresponding author**: Daniel E. Spratt, MD, Department of Radiation Oncology, Memorial Sloan-Kettering Cancer Center, 1275 York Avenue, Box 22, New York, NY 10065; sprattd@mskcc.org.

Dr. Yamada is a Consultant for Varian Medical Systems, Inc. and a member of the Speakers Bureau for the Institute for Medical Education; the other authors have no financial disclosures or conflicts of interest to report.

Methods—All measurements were independent and blinded by two neuroradiologists. R2 statistics were performed to document correlation, and two-tailed t-tests were used to compare groups. P<0.05 was deemed statistically significant.

Results—The median time from SBRT until post-treatment MRI was 57 days. Local failure developed in one lesion (8.3%) 10 months after SBRT. Vp mean, Ktrans mean, Vp max, and Ktrans max were significantly decreased post-SBRT as compared to pre-SBRT (58.7%, 63.2%, 59.0%, and 55.2%; all p-values <0.05). Bi-dimensional tumor measurements demonstrated an average increase in size across the cohort, and 50%, 25%, and 25% of the treated lesions demonstrated features of "worsening," "no change," or "improvement," respectively, by both radiologists' graded impressions. There was good inter-reader reliability for both size and subjective disease response scores (R^2 = 0.84). The mpMRI score had 100% accuracy in predicting local control at time of last follow-up. There was no apparent correlation with size changes compared to the mpMRI score change post-SBRT (R^2 = 0.026).

Conclusions—We report the first analysis on the utility of DCE-MRI for metastatic sarcoma spine metastases treated with SBRT. We demonstrate that early assessment at two months post-SBRT using size and subjective neuroradiology impressions is insufficient to judge ultimate disease progression, and that a combination of perfusion parameters provides excellent correlation to local control.

Keywords

Spine; Radiotherapy; Stereotactic radiotherapy; Sarcoma; Metastases; MRI; Imaging

INTRODUCTION

Sarcomas are an uncommon form of cancer representing only 0.7% (n=15,040) of all newly diagnosed cancer cases in the United States each year.[1] Development of metastatic disease is dependent on histology, and long-term incidence of metastatic disease for soft-tissue sarcomas of the extremity is approximately 20%.[2] Metastatic sarcoma to the spine is extremely rare and portends a dire prognosis. It is therefore difficult to study this cohort of patients and novel therapeutic options are needed.

Metastatic disease to vertebral bodies can result in pain and deterioration in quality of life.[3] The involvement of adjacent nerve roots or the spinal cord itself can lead to life-threatening neurological symptoms.[4] Palliative therapies such as radiotherapy have historically had limited success in controlling sarcomas near the spine due to their radioresistant phenotype and nearby essential normal structures.[5] In the past decade, there has been a surge of advances in image-guided and stereotactic body radiotherapy (SBRT) that have allowed for high single and hypofractionated courses of radiotherapy.[5, 6] This technological advance has resulted in unprecedented rates of 1-year local tumor control upwards of 85%.[6] Effective measures are needed to assess those patients who will experience local failure after SBRT, particularly given the improved prognosis of many of these patients with advances in systemic therapy.

Dynamic contrast-enhanced MRI (DCE-MRI) is a potential predictor of treatment response that utilizes quantitive metrics.[7, 8] This is in stark contrast to traditional subjective reads that rely on reader expertise and demonstrate greater inter-reader variability. In addition, when monitoring response to SBRT to vertebral bodies, significant post-treatment effects and changes to the bone make common response criteria such as RECIST difficult to implement.[9]

Given the poor prognosis of patients with metastatic sarcoma to the spine and the difficulty in assessing early response, we herein report the results of 12 consecutively treated lesions from patients with metastatic sarcoma to the spine that underwent pre- and post-SBRT DCE-MRI and correlate various radiologic metrics to long-term outcome.

METHODS

Patient Details

After institutional review board approval, our center's sarcoma spine database of 240 patients was queried to identify eligible patients. Criteria for inclusion were patients who were treated with SBRT and were imaged pre- and post-treatment with DCE-MRI. We excluded patients who underwent surgical resection prior to RT. Nine patients were identified that were treated with SBRT to 12 independent spinal lesions.

All patients had histologic confirmation and pathology review at our institution. Pre- and post-treatment imaging were performed at our institution and read by a board-certified neuroradiologist. A multidisciplinary team of experts in spinal malignancy comprising a neurosurgeon, radiation and medical oncologists, interventional radiologists, and neuroradiologists reviewed each case prior to administration of SBRT and utilized the NOMS [Neurologic Oncologic Mechanical Instability Systemic Disease] framework for clinical decision making.[10]

Simulation, Treatment Planning, and Radiotherapy Details

Hypofractionated and single-fraction SBRT techniques were performed as previously described.[11] In brief, patients were immobilized in our custom institutionally-made cradle. Patients underwent a myelogram prior to CT simulation for improved visualization of the spinal canal. CT simulation utilized 2-mm slice thickness. The Spratt Six Segmentation System was utilized for target delineation as per the International Spine Radiosurgery Consortium consensus guidelines.[12] Dose constraints have been previously reported.[11] Treatments were delivered with 7 to 11 coplanar fields with dynamic multi-leaf collimation. The dose was prescribed to the 100% isodose line in all cases. A mix of 6 and 15 MV beam energies was most commonly used. A cone beam CT was used for image guidance and orthogonal KV imaging was obtained for each fraction to verify the patient position.

DCE-MRI Details

All patients underwent a pre-SBRT assessment with a DCE-MRI of the total spine. The median time from SBRT completion to post-treatment DCE-MRI was 57 days (interquartile range, 51–62 days, range 42–79 days). MRI sequences of the spine were acquired with a

1.5-T GE scanner (Milwaukee, Wisconsin) using an 8-channel cervical-thoracic-lumbar (CTL) surface coil. All patients underwent routine MRI, including sagittal T1 (field-of-view [FOV], 32–36 cm; slice thickness, 3 mm; repetition time [TR], 400–650ms; flip angle [FA], 90°), T2 (FOV, 32–36 cm; slice thickness, 3 mm; TR, 3500–4000ms; FA, 90°), and sagittal short inversion time inversion recovery [STIR] (FOV, 32–36 cm; slice thickness, 3 mm; TR, 3500–6000ms; FA, 90°).

DCE-MRI of the spine was then acquired. A bolus of gadolinium-diethylenetriamine penta-acetic acid (Gd-DTPA) was administered by a power injector at 0.1 mmol/kg body weight and a rate of 2 to 3 mL/sec. The kinetic enhancement of tissue during and after injection of Gd-DTPA was obtained using a 3D T1-weighted fast spoiled-gradient (SPGR) echo sequence (TR, 4–5 ms; echo time [TE], 1–2 seconds; slice thickness, 5 mm; FA, 25°; FOV, 32cm; temporal resolution (Δt) of 6.5 ms) and consisted of 10–12 images in the sagittal plane. The 3D SPGR sequences generated phase images in addition to the standard magnitude images. The duration of the DCE sequence was 300 seconds. Sagittal and axial T1-weighted post-Gd-DTPA MR images were acquired after DCE-MRI.

Processing and analysis of perfusion raw data was performed using FDA-approved available image processing software (NordicIce-NeuroLab, Bergen, Norway). Pre-processing comprised background spatial and temporal smoothing, noise removal, and detection of the arterial input function (AIF) from the aorta. AIF was calculated in each acquisition of every patient. Optimal shape of the AIF curve was selected before processing steps continued. Linear assumption between change in signal intensity and gadolinium concentration was made to convert the signal intensity curve to the concentration-time curve. The Tofts 2-compartment pharmacokinetic model analysis was used for the calculation of quantitative perfusion parameters, including time-dependent leakage (Ktrans) and blood plasma volume (Vp).[13] Regions of interest (ROIs) were placed in metastatic deposits on the parametric maps by a radiologist, who was blinded to clinical outcome, with special consideration to avoid normal-appearing marrow, lesion margins, endplates, spondylotic changes, and vessels (specifically the basivertebral venous plexus). Anatomical T1-weighted pre-contrast and STIR sequences matching the DCE-MRI maps were used for optimal ROI placements. Parameters were normalized to a ratio of lesion-to-normal marrow value by selecting ROIs in normal marrow of adjacent healthy-looking vertebral bodies, excluding vertebral bodies with post-radiation or abnormal signal changes.

Imaging Analysis

Conventional metrics to assess treatment response were performed by two independent and blinded board-certified neuroradiologists. Conventional metrics included a bi-dimension measurement of tumor size and a three-tiered subjective scoring system (“worsening of disease,” “no change,” or “improvement”).

For quantitative parameters, including assessment of the time-dependent leakage constant (Ktrans) and blood plasma volume (Vp), both mean and max values were calculated. Percent change from pre-SBRT to post-treatment was calculated for all parameters.

Endpoint Definitions and Statistics

Local failure was defined as a progressive radiographic increase in size of the treated lesion with consideration of the clinical scenario such as progression of neurologic symptoms referable to the treated site. As evident from our present analysis (i.e., lesions 6, 7, 8, 10, and 11), treated lesions often increase in size immediately post-treatment so local failure was not coded unless there was persistent progression on more than one post-treatment scan or documentation from a biopsy (one lesion was biopsied). Local progression was made by a consensus from the multidisciplinary spine team.

A composite mpMRI score was created as a simple geometric average of the four perfusion parameters (Vp max, Vp mean, Ktrans max, and Ktrans mean). Correlations using R^2 statistics were performed to correlate inter-reader reliability, as well as to correlate metrics of bi-dimensional tumor size changes with the mpMRI score. Changes in perfusion parameters from SBRT were compared using a paired t-test. Two-sided *P* values of ≤ .05 were considered statistically significant. Statistical analysis was performed using SPSS version 21 (SPSS, Inc, USA).

RESULTS

The median follow-up of our cohort was 11.2 months (range, 5.1–31.1 months). The median age of our cohort was 61 years old (range, 33–77), and the majority of lesions treated were from female patients (67%). Fifty percent of patients had their sarcoma originate from the abdomen or pelvis, 17% from the head and neck, and 33% from the extremities. A wide variety of sarcoma histologic subtypes were treated (Table 1), with the most common being leiomyosarcoma (50%). The majority of patients had a good performance status, with 83% having a Karnofsky Performance Status (KPS) of 80. All patients in our cohort had multiple sites of metastatic disease, and 83% of patients had both bone and visceral metastases. The lumbar spine was the most common site of metastatic disease (67%), and both the thoracic spine and sacrum were involved in 17% of the cohort.

Fifty percent of lesions were treated with 24 Gy in a single fraction, 33% were treated to a total dose of 27 Gy (9 Gy×3 fractions), and one patient was treated to 30 Gy (10 Gy×3 fractions). The median BED was 81.6 Gy (range, 51.3–81.6 Gy). The median GTV volume was 6.6 cm^3 (range, 1.0–46.5) and the median PTV volume was 115.1 cm^3 (range, 7.6–203.2). Systemic therapy was administered to 83% of the cohort post-SBRT. Only one patient experienced a local failure 10.2 months post-SBRT, and lived a total of 13.8 months post-SBRT.

Conventional MR Metrics

The average bi-dimensional size pre-treatment for reader 1 and reader 2 was 5.7 cm^2 and 4.4 cm^2, respectively, and the average area post-treatment for reader 1 and reader 2 was 6.1 cm^2 and 6.4 cm^2, respectively. The average percent change from SBRT was an increase of 2.2% and 5.1% for reader 1 and reader 2, respectively. There was good inter-reader reliability in the tumor measurements (R^2 = 0.84, Table 2 and Figure 1).

The accuracy of conventional MR size metrics were compared to that of the mpMRI score. A waterfall plot (Figure 2a) demonstrated that all but one lesion (92%) demonstrated a decrease in the mpMRI score, whereas six lesions (50%) demonstrated a decrease in size post-SBRT. There was no apparent correlation with size changes compared to the mpMRI score change post-SBRT ($R^2 = 0.026$, Figure 2b).

Lesions 6, 7, 8, 10, and 11 initially showed an increase in size, and then showed a decrease in lesion size on subsequent imaging, indicative of pseudoprogression.

DCE-MRI Analysis

Quantitative perfusion parameters (Vp mean, Vp max, Ktrans mean, and Ktrans max) were significantly decreased post-SBRT; 58.7%, 63.2%, 59.0%, and 55.2%; p=0.006, 0.02, 0.001, and 0.005, respectively (Table 2 and Figure 3a). Ninety-two percent of lesions had a reduction in Vp mean and Vp max post-SBRT; however, the single lesion that had an increase in both parameters did not develop a local failure and did not increase in size or progress by subjective neuroradiology impression. Ktrans mean decreased in 75% of lesions, with two lesions demonstrating an increase that did not develop local recurrence, and one lesion that did progress clinically. Ktrans max decreased in 92% of patients, with the one patient who had an increase also developing a recurrence. Overall, Ktrans max had 100% accuracy in predicting later failure. When utilizing the mpMRI score, a composite average of all perfusion parameters, there was also 100% accuracy in predicting local failure (Figure 3b). A representative visual example of the decrease in Vp is shown in Figure 4.

DISCUSSION

Non-invasive methods for early detection of treatment outcome are crucial, especially when tumors are located near critical structures such as the spinal axis, where a delay in intervention can result in serious sequelae such as paralysis. Herein, we report the first and largest series of patients with metastatic spinal sarcoma assessed by pre- and post-SBRT DCE-MRI, and demonstrated that traditional metrics such as subjective neuroradiologist impression and bi-dimensional size measurements are insufficient to assess future progression of disease. Conversely, perfusion parameters including Ktrans and Vp appear to provide accurate predictions of early treatment failure.

Conventional metrics to judge treatment response, including RECIST, are difficult to apply for spinal tumors due to a multitude of post-treatment changes that occur.[14] Radiotherapy is known to cause necrosis and fibrosis of tumor and surrounding adjacent normal tissue, which can result in what appears as worsening of disease on imaging.[15] This is a well documented phenomenon in other tumor sites such as brain metastases when treated with single fraction radiosurgery, which can occur at rates of ~10% in the first year post-treatment. This can often impose significant clinical uncertainty to whether progression has occurred.[16] Further complicating standard metrics for evaluating treatment success include vertebral body collapse or more subtle osseous changes post-SBRT.[9] However, no patients in our study had suffered a vertebral body collapse at the time of the initial post-SBRT MRI. Estimated rates of vertebral body compression fracture after SBRT typically range from 11–39%, and are likely related to the total biologically effective dose delivered.[17] This is in

contrast to conventional radiotherapy doses, which cause vertebral compression fractures in less than 5% of patients. When vertebral body compression/collapse occurs, it can cause tumor measurements to be less reliable. Lastly, another limitation of standard MR metrics for radiation-resistant histologies are that most of these histologies uncommonly undergo apoptosis and are unlikely to rapidly resolve post-SBRT. This is in contrast to radiosensitive histologies such as multiple myeloma where complete resolution of the tumor is routine post-radiotherapy.[18]

DCE-MRI with Gd-DTPA has been used to measure perfusion in many tumor types, as well as perfusion of organs such as the heart, bone, and brain.[8, 19–21] To our knowledge, this is the first study to evaluate the use of DCE-MRI to assess changes in perfusion for sarcoma neoplasms in response to SBRT. In our study we found that both Ktrans and Vp were more accurate in predicting ultimate tumor control than the subjective neuroradiology scale or size measurements. Ktrans estimates the velocity of blood transfer from the vascular compartment to the interstitial space, and is commonly used for assessing vascular perfusion properties in various organ sites.[22] Ktrans appeared to be modestly more accurate than Vp in predicting treatment success; however, due to the limited sample size and event rate, this should be interpreted with caution.

Vp is a measure of intravascular volume, and the decrease in Vp and Ktrans that we observed in nearly all tumors is likely related to the underlying destruction of tumor vasculature. A wealth of preclinical data supports the notion that high-dose radiotherapy causes apoptosis through ceramide/sphingomyelinase pathways of tumor vasculature, which ultimately results in tumor death.[23] Thus, perfusion metrics are likely of even more biological relevance when judging treatment response to SBRT, in comparison to conventionally fractionated radiotherapy. The increase in Ktrans in the tumor that ultimately experienced a local failure may indicate resistance to this mode of cell death or perhaps is related to the secretion of angiogenic factors by the tumor or microenvironment supporting increased perfusion for future growth.

The primary strength of our study is the homogeneity of our patient population—all patients had metastatic sarcoma, which is a radioresistant tumor. Furthermore, nearly all patients had a DCE- MRI within two months post-SBRT, allowing for judgment of early treatment success before the clinical outcome was known. Additionally, all lesions were assessed through multiple metrics, both qualitative and quantitative, by two independent expert neuroradiologists who were blinded to the treatment outcome. However, our study has limitations. First, the study was retrospective, which may subject the results to bias that could not be fully accounted for. Second, as MR imaging was not performed the day of SBRT start, it is difficult to account for any potential tumor size changes from pre-treatment imaging until SBRT start. Third, despite this being an exceedingly rare disease entity, our sample size is still limited, and due to the success of SBRT, only one patient had a local failure in this series. Despite these limitations, we believe the results of the present study should be hypothesis-generating for further study to assess the importance and utility of early assessment of perfusion parameters.

CONCLUSION

We report the first analysis on the utility of T1-weighted DCE-MRI for metastatic sarcoma spine metastases treated with SBRT. We demonstrate that early assessment at two months post-SBRT of traditional subjective impressions and size criteria alone are insufficient to judge ultimate disease progression, and that a combination of perfusion parameters provides excellent correlation to local control. The utility of DCE-MRI should be further investigated in a prospective cohort in other metastatic spinal radioresistant tumors treated with SBRT.

References

1. Siegel R, Ma J, Zou Z, Jemal A. Cancer statistics, 2014. CA: a cancer journal for clinicians. 2014; 64(1):9–29. [PubMed: 24399786]
2. Yang JC, Chang AE, Baker AR, et al. Randomized prospective study of the benefit of adjuvant radiation therapy in the treatment of soft tissue sarcomas of the extremity. Journal of Clinical Oncology. 1998; 16(1):197–203. [PubMed: 9440743]
3. Sze WM, Shelley M, Held I, Wilt T, Mason M. Palliation of metastatic bone pain: single fraction versus multifraction radiotherapy–a systematic review of randomised trials. Clinical Oncology. 2003; 15(6):345–352. [PubMed: 14524489]
4. Desforges JF, Byrne TN. Spinal cord compression from epidural metastases. New England Journal of Medicine. 1992; 327(9):614–619. [PubMed: 1296600]
5. Gerszten PC, Mendel E, Yamada Y. Radiotherapy and radiosurgery for metastatic spine disease: what are the options, indications, and outcomes? Spine. 2009; 34(22S):S78–S92. [PubMed: 19829280]
6. Yamada Y, Bilsky MH, Lovelock DM, et al. High-dose, single-fraction image-guided intensity-modulated radiotherapy for metastatic spinal lesions. International Journal of Radiation Oncology* Biology* Physics. 2008; 71(2):484–490.
7. O'Connor JP, Jackson A, Parker GJ, Jayson GC. DCE-MRI biomarkers in the clinical evaluation of antiangiogenic and vascular disrupting agents. British journal of cancer. 2007; 96(2):189–195. [PubMed: 17211479]
8. Yankeelov TE, Lepage M, Chakravarthy A, et al. Integration of quantitative DCE-MRI and ADC mapping to monitor treatment response in human breast cancer: initial results. Magnetic resonance imaging. 2007; 25(1):1–13. [PubMed: 17222711]
9. Cunha MV, Al-Omair A, Atenafu EG, et al. Vertebral compression fracture (VCF) after spine stereotactic body radiation therapy (SBRT): analysis of predictive factors. International Journal of Radiation Oncology* Biology* Physics. 2012; 84(3):e343–e349.
10. Fisher CG, DiPaola CP, Ryken TC, et al. A novel classification system for spinal instability in neoplastic disease: an evidence-based approach and expert consensus from the Spine Oncology Study Group. Spine. 2010; 35(22):E1221–E1229. [PubMed: 20562730]
11. Folkert MR, Bilsky MH, Tom AK, et al. Outcomes and Toxicity for Hypofractionated and Single-Fraction Image-Guided Stereotactic Radiosurgery for Sarcomas Metastasizing to the Spine. International Journal of Radiation Oncology* Biology* Physics. 2014; 88(5):1085–1091.
12. Cox BW, Spratt DE, Lovelock M, et al. International Spine Radiosurgery Consortium consensus guidelines for target volume definition in spinal stereotactic radiosurgery. International Journal of Radiation Oncology* Biology* Physics. 2012; 83(5):e597–e605.
13. Tofts PS, Brix G, Buckley DL, et al. Estimating kinetic parameters from dynamic contrast-enhanced T1-weighted MRI of a diffusable tracer: standardized quantities and symbols. Journal of Magnetic Resonance Imaging. 1999; 10(3):223–232. [PubMed: 10508281]
14. Eisenhauer E, Therasse P, Bogaerts J, et al. New response evaluation criteria in solid tumours: revised RECIST guideline (version 1.1). European journal of cancer. 2009; 45(2):228–247. [PubMed: 19097774]

15. Brandes AA, Tosoni A, Spagnolli F, et al. Disease progression or pseudoprogression after concomitant radiochemotherapy treatment: pitfalls in neurooncology. Neuro-oncology. 2008; 10(3):361–367. [PubMed: 18401015]
16. Stockham AL, Chao ST, Suh JH. Wanted: Dead or alive? Distinguishing radiation necrosis from tumor progression after stereotactic radiosurgery.
17. Sahgal A, Whyne CM, Ma L, Larson DA, Fehlings MG. Vertebral compression fracture after stereotactic body radiotherapy for spinal metastases. The lancet oncology. 2013; 14(8):e310–e320. [PubMed: 23816297]
18. Wood AJ, Alexanian R, Dimopoulos M. The treatment of multiple myeloma. New England Journal of Medicine. 1994; 330(7):484–489. [PubMed: 8289856]
19. Walker-Samuel S, Leach M, Collins D. Evaluation of response to treatment using DCE-MRI: the relationship between initial area under the gadolinium curve (IAUGC) and quantitative pharmacokinetic analysis. Physics in medicine and biology. 2006; 51(14):3593. [PubMed: 16825751]
20. Sourbron S, Ingrisch M, Siefert A, Reiser M, Herrmann K. Quantification of cerebral blood flow, cerebral blood volume, and blood–brain-barrier leakage with DCE-MRI. Magnetic Resonance in Medicine. 2009; 62(1):205–217. [PubMed: 19449435]
21. Lee JH, Dyke JP, Ballon D, Ciombor DM, Tung G, Aaron RK. Assessment of bone perfusion with contrast-enhanced magnetic resonance imaging. Orthopedic Clinics of North America. 2009; 40(2):249–257. [PubMed: 19358910]
22. Dyke J, Aaron R. Noninvasive methods of measuring bone blood perfusion. Annals of the New York Academy of Sciences. 2010; 1192(1):95–102. [PubMed: 20392223]
23. Verheij M, Bose R, Lin XH, et al. Requirement for ceramide-initiated SAPK/JNK signalling in stress-induced apoptosis. 1996

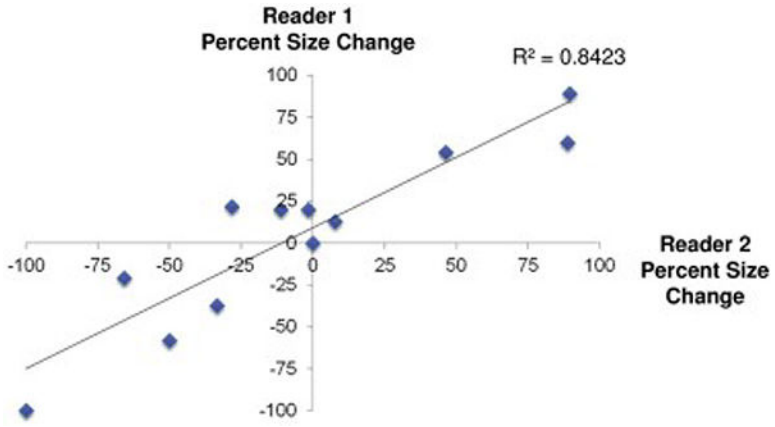

Figure 1.

Scatter plot of inter-reader reliability of bi-dimensional size measurements between two independent neuroradiologists. There is excellent correlation between readers ($R^2 = 0.84$).

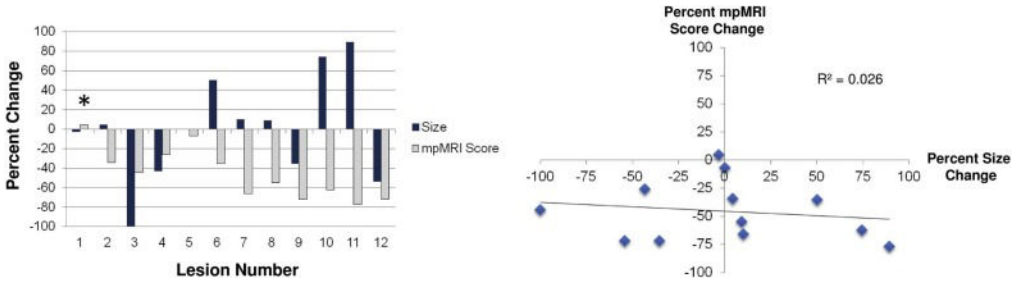

Figure 2.

Correlation between size changes and changes in the mpMRI score. A) Waterfall plot of mpMRI co-plotted with size change. B) Scatter plot demonstrating no correlation between size and mpMRI ($R^2 = 0.026$).

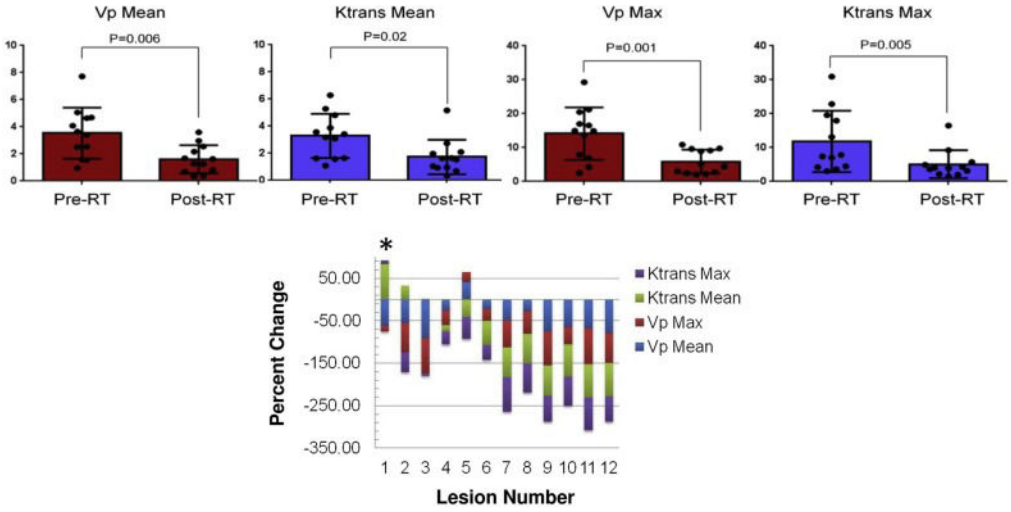

Figure 3.

Change in perfusion parameters Vp and Ktrans mean and max post-SBRT. A) As a cohort, all parameters demonstrate a significant decrease post-SBRT. B) Individual waterfall plot of all parameters and their relative percent change post-SBRT. Patient 1, who developed a local failure, demonstrated an increase in Ktrans mean and max and had small reductions in Vp max. *Indicates patient who experienced a local failure.

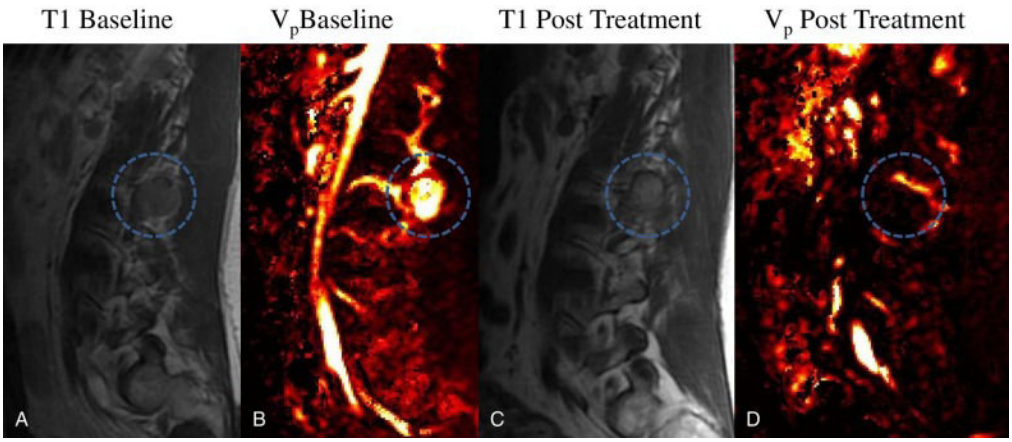

Figure 4.

Example of patient treated with SBRT for a lumbar paraspinal mass. Sagittal T1 pre-contrast and Vp images, pre-treatment (left) and post-SBRT (right), demonstrate minimal reduction in tumor size but complete visual absence of perfusion.

Table 1

Baseline and Treatment Characteristics

			n=	%
Age				
	median	(range)	61	(33–77)
Gender				
	Male		4	33
	Female		8	67
Primary Tumor site				
	Head/Neck		2	17
	Abdomen/Pelvis		6	50
	Extremeties		4	33
Histology				
	Hemangiopericytoma		2	17
	Rhabdomyosarcoma		1	8
	Leiomyosarcoma		6	50
	Myxoid Fibrosarcoma		2	17
	Myxoid Liposarcoma		1	8
KPS				
	80		10	83
	90		2	17
Disease Extent at Spine RT Start				
	Single metastatic site		0	0
	Disseminated spine/bone only		2	17
	Bone and Visceral sites		10	83
Treated Spinal Site				
	Thoracic Spine		2	17
	Lumbar Spine		8	67
	Sacrum		2	17
RT Dose x Fraction				
	24 Gy x 1		7	58
	9 Gy x 3		4	33
	10 Gy x 3		1	8
BED				
	Median	(range)	81.6	(51.3–81.6)
GTV Volume (cm3)				
	Median	(range)	6.6	(1.0–46.5)
PTV Volume (cm3)				
	Median	(range)	115.1	(7.6–203.2)
Systemic Therapy Post-RT				
	Yes		10	83
	No		2	17

Table 2

MR imaging analyses post-SBRT

	Multiparametric quantitative metrics						Subjective Score		Quantitative Size Measurements (cm)				
									Reader 1		Reader 2		
Lesion ID	Local Progression	Vp mean (% change)	Vp max (% change)	Ktrans mean (% change)	Ktrans max (% change)	mp MRI Score (% change)	Reader 1	Reader 2	Pre-RT	Post-RT	Pre-RT	Post-RT	Total Follow-up post-SBRT (months)
1	Yes	− 62.3	−12.2	83.4	9.5	4.6	Worse	Worse	1.9 × 2.9	2.2 × 1.8	1.9 × 1.9	2.2 × 2.0	13.8
2	No	−55.2	−68.9	33.3	−46.7	−34.4	No Change	No Change	1.8 × 1.3	1.6 × 1.3	1.5 × 1.3	1.8 × 1.3	15.6
3	No	−91.2	−82.3	2.8	−6.9	− 44.4	Improved	Improved	2.7 × 2.3	0 × 0	2.7 × 2.3	0 × 0	5.1
4	No	−25.5	−35.3	−14.4	−29.7	−26.2	Improved	Improved	2.4 × 2.2	1.8 × 1	2.4 × 2.2	2.2 × 1.9	8.3
5	No	41.6	23.0	−41.5	−51.5	−7.1	No Change	No Change	2.6 × 2.6	2.6 × 2.6	2.6 × 2.6	2.6 × 2.6	8.4
6	No	−22.3	−27.2	−57.6	−34.5	−35.4	Worse	Worse	6.1 × 2.7	7.3 × 3.3	6.1 × 2.6	7.4 × 3.3	11.2
7	No	−48.4	−64.9	−68.8	−82.4	−66.1	Worse	No Change	4.5 × 1.7	4.2 × 3.5	4.3 × 2.6	4.5 × 2.8	10.6
8	No	−27.3	−53.1	−69.8	−68.6	−54.7	Worse	Worse	4.0 × 2.8	3.8 × 2.9	4.0 × 2.8	4.8 × 2.8	8.6
9	No	−75.3	−79.1	−72.1	−60.3	−71.7	Improved	Improved	1.5 × 1.3	1.3 × 1.0	1.6 × 1.3	1.3 × 1.0	8.1
10	No	−64.3	−41.1	−75.7	−68.1	−62.3	Worse	Worse	1.3 × 1.1	1.8 × 1.5	1.5 × 1.2	1.8 × 1.6	12.5
11	No	−68.3	−83.8	−78.2	−78.1	−77.1	Worse	Worse	1.9 × 1.2	2.4 × 1.8	1.9 × 1.2	2.4 × 1.8	12.3
12	No	−78.6	−71.0	−78.6	−58.8	−71.8	Improved	Improved	1.2 × .9	0.9 × 0.6	1.2 × 0.9	0.9 × 0.5	31.1